AGU PUBLICATIONS

Geophysical Research Letters

RESEARCH LETTER
10.1002/2017GL073355

Key Points:
- There will be significant decrease in the transport of NMK system that is attributed to the weakened north-easterly trade winds
- The zero wind stress curl line and NEC bifurcation shift northward under global warming
- There will be a robust increase in both the seasonal south-north migration of zero curl line and NEC bifurcation under global warming

Supporting Information:
- Supporting Information S1

Correspondence to:
Z. Chen,
chenzhaohui@ouc.edu.cn

Citation:
Duan, J., Z. Chen, and L. Wu (2017), Projected changes of the low-latitude north-western Pacific wind-driven circulation under global warming, *Geophys. Res. Lett.*, *44*, doi:10.1002/2017GL073355.

Received 7 MAR 2017
Accepted 26 APR 2017
Accepted article online 27 APR 2017

Projected changes of the low-latitude north-western Pacific wind-driven circulation under global warming

Jing Duan[1,2], Zhaohui Chen[1,2], and Lixin Wu[1,2]

[1]Physical Oceanography Laboratory, CIMST, Ocean University of China, Qingdao, China, [2]Qingdao National Laboratory for Marine Science and Technology, Qingdao, China

Abstract Based on the outputs of 25 models participating in the Coupled Model Intercomparison Project Phase 5, the projected changes of the wind-driven circulation in the low-latitude north-western Pacific are evaluated. Results demonstrate that there will be a decrease in the mean transport of the North Equatorial Current (NEC), Mindanao Current, and Kuroshio Current in the east of the Philippines, accompanied by a northward shift of the NEC bifurcation Latitude (NBL) off the Philippine coast with over 30% increase in its seasonal south-north migration amplitude. Numerical simulations using a 1.5-layer nonlinear reduced-gravity ocean model show that the projected changes of the upper ocean circulation are predominantly determined by the robust weakening of the north-easterly trade winds and the associated wind stress curl under the El Niño-like warming pattern. The changes in the wind forcing and intensified upper ocean stratification are found equally important in amplifying the seasonal migration of the NBL.

1. Introduction

The low-latitude north-western Pacific is a key region for global climate, owing to its residence in the western Pacific warm pool and important role in meridional redistribution of heat, moisture, and mass. The upper ocean circulation system (Figure 1a) composed by the east-west North Equatorial Current (NEC), the northward flowing Kuroshio Current (KC), and the southward flowing Mindanao Current (MC), has been paid much attention over the past three decades. On the one hand, the water masses transported by MC feed the tropical circulation cells and the Indonesian Throughflow (ITF), influencing the evolution of El Niño–Southern Oscillation (ENSO) and regulating the regional/global climate [*Lukas et al.*, 1991, 1996; *Gu and Philander*, 1997; *Johnson and Mcphaden*, 1999; *Gordon et al.*, 2003; *Kashino et al.*, 2005; *Wittenberg et al.*, 2006; *Kashino et al.*, 2009; *Hsin and Qiu*, 2012; *Sprintall et al.*, 2014; *Rudnick et al.*, 2015; *Schönau et al.*, 2015; *Sen Gupta et al.*, 2016]. On the other hand, the Kuroshio, originating to the east of the Philippines due to the bifurcation of NEC, carries warm water to downstream regions of colder air temperature, supplying heat, and moisture to the atmosphere along its paths [*Kelly et al.*, 2010; *Kwon et al.*, 2010; *Sasaki et al.*, 2012].

In addition to in-depth studies of multitimescale variability of this current system [*Hu and Cui*, 1989; *Qiu and Lukas*, 1996; *Yaremchuk and Qu*, 2004; *Kashino et al.*, 2009; *Zhai et al.*, 2014], its response to increasing greenhouses gases under global warming is of importance as we assess the global warming impact on the ocean circulation. Recently, our knowledge of projected changes in the tropical Pacific Ocean circulation has been gradually enriched in the aid of coupled models participated in the Coupled Model Intercomparison Project (CMIP) [e.g., *Sen Gupta et al.*, 2012; *Hu et al.*, 2015; *Sen Gupta et al.*, 2016]. In the tropical Pacific, particularly in the equatorial regions, *Sen Gupta et al.* [2012] suggested a significant decrease in the mean state transport of the MC at 9°N and Indonesian Throughflow and an increase in the transport of the Equatorial Undercurrent and New Guinea Coastal Undercurrent. A recent comprehensive study by *Hu et al.* [2015] systematically reveals the projected changes in these currents associated with greenhouse-gas-induced climate change. It is shown that compared with historical mean, the averaged upstream KC (15°N–25°N) is projected to decrease by approximately 10% over 2050–2100 under Representative Concentration Pathway (RCP) 8.5 scenario, so are the MC (5°N–10°N) and NEC (170°E) (they are projected to weaken by 3 sverdrup (Sv) and 6 Sv, respectively; 1 Sv = 10^6 m^3 s^{-1}). Although the general response of NEC-KC-MC system (also known as NKM) to global warming is relatively well understood, detailed future changes especially the projected NEC bifurcation latitude (NBL) remain unclear.

In this paper, we will demonstrate primarily the projected changes of the NKM system, focusing on the mean and seasonal variations of the NBL. In section 2, we give a brief description of the model data and

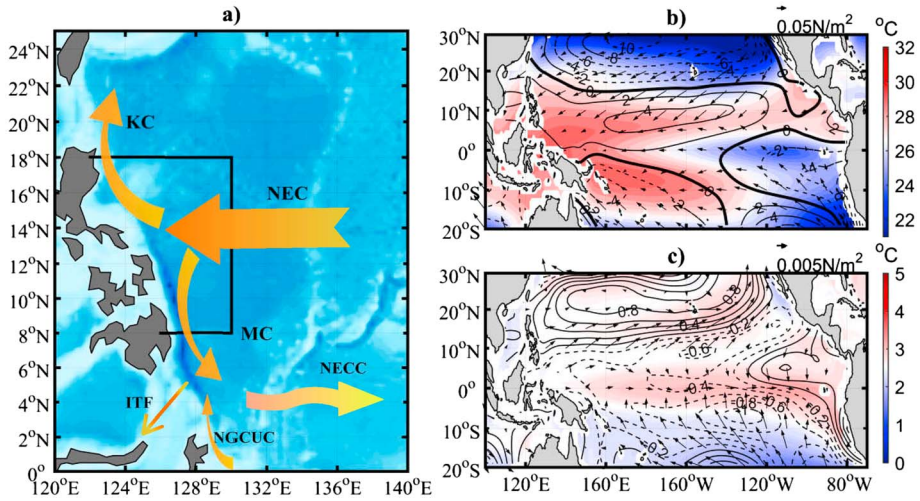

Figure 1. (a) Major low-latitude north-western Pacific currents. NEC, North Equatorial Current; KC, Kuroshio Current; MC, Mindanao Current; ITF, Indonesian Throughflow; NGCUC, New Guinea Coastal Undercurrents (black box shows the location of the NEC-KC-MC system sections). (b) MMM SST (shading), wind stress (vectors), and wind stress curl (contours; unit: 1×10^{-8} N m^{-3}) averaged over the 1951–2000 period. (c) MMM projected change (2051–2100 minus 1951–2000) in SST (shading), wind stress (vectors), and wind stress curl (contours; unit: 1×10^{-8} N m^{-3}).

methodology, followed by the results in section 3. Possible mechanisms related to the projected changes are examined in section 4. Section 5 provides the summary.

2. Data and Method

To assess the future changes of the wind-driven circulation in the low-latitude north-western Pacific, we analyzed the outputs from 25 CMIP Phase 5 (CMIP5) models. All the model runs are derived from the r1i1p1 run.

Table 1. 25 Models From CMIP5 Used in This Study

Model Name	Nation	Horizontal Resolution of Atmospheric Model	Horizontal Resolution of Ocean Model
ACCESS1–0	Australia	1.241° × 1.875°	0.6° × 1°
ACCESS1–3	Australia	1.241° × 1.875°	0.6° × 1°
CanESM2	Canada	2.813° × 2.813°	1.41° × 0.94°
CCSM4	USA	0.938° × 1.25°	0.469° × 1.125°
CESM1-BGC	USA	0.938° × 1.25°	0.469° × 1.125°
CMCC-CESM	Italy	3.75° × 2.5°	1.208° × 1.978°
CMCC-CM	Italy	0.75° × 0.75°	1.208° × 1.978°
CMCC-CMS	Italy	1.875° × 1.25°	1.208° × 1.978°
CNRM-CM5	France	1.406° × 1.406°	0.616° × 0.995°
CSIRO-Mk3–6-0	Australia	1.875° × 1.875°	0.952° × 1.875°
GFDL-CM3	Unite States	2° × 2.5°	0.9° × 1°
GFDL-ESM2M	Unite States	2° × 2.5°	0.9° × 1°
GISS-E2-R	USA	2° × 2.5°	2° × 2.5°
GISS-E2-R-CC	USA	2° × 2.5°	2° × 2.5°
HadGEM2-CC	Unite Kingdom	1.241° × 1.875°	0.833° × 1°
HadGEM2-ES	Unite Kingdom	1.241° × 1.875°	0.833° × 1°
IPSL-CM5A-LR	France	1.875° × 3.75°	1.208° × 1.978°
IPSL-CM5A-MR	France	1.208° × 2.5°	1.208° × 1.978°
IPSL-CM5B-LR	France	1.875° × 3.75°	1.208° × 1.978°
MIROC-ESM	Japan	2.813° × 2.813°	0.938° × 1.406°
MIROC-ESM-CHEM	Japan	2.813° × 2.813°	0.938° × 1.406°
MPI-ESM-LR	Germany/Korea	1.208° × 1.875°	1.818° × 1.406°
MPI-ESM-MR	Germany/Korea	1.875° × 1.875°	0.446° × 0.449°
MRI-CGCM3	Japan	1.125° × 1.125°	0.489° × 1°
NorESM1-M	Norway	1.875° × 2.5°	0.469° × 1.125°

The model names and resolutions are summarized in Table 1. More details for the CMIP5 models can be found at http://cmip-pcmdi.llnl.gov/cmip5/. In the following analysis, we used the monthly mean horizontal current (*u* and *v*), zonal and meridional wind stress (*taux* and *tauy*), and sea surface temperature (SST). To facilitate analysis, all the variables are interpolated onto a 0.25° × 0.25° grid.

In this study, the transport of NEC, MC, and KC is defined as the volume transport above 400 m integrated along 8°N–18°N, 130°E for NEC, from the Mindanao coast to 130°E at 8°N for MC, and from the Luzon coast to 130°E at 18°N for KC (Figure 1a). The NBL is defined as the latitude where the meridional velocity averaged over the upper 400 m within 2° band off the Philippine coast is zero [*Qiu and Lukas*, 1996; *Chen and Wu*, 2012].

3. Results

3.1. Projected Changes of the Mean State

Before we go into the projected changes of the current system, it is useful to first illustrate the future patterns of the large-scale SST and winds over the entire tropical Pacific in the emission scenarios of greenhouse gases. Figure 1b shows the multimodel mean (MMM) field of the tropical Pacific from historical runs. The overall patterns of SST and wind stress are generally consistent with observations [e.g., *Osamu and Akio*, 2004; *Wu and Xie*, 2013]. The difference of wind stress between historical runs and RCP8.5 runs (i.e., 2051–2100 minus 1951–2000) is shown in Figure 1c. The low-latitude Pacific Ocean is dominated by a robust weakening of the north-easterly trade winds and resultant wind stress curl changes on both sides. Quantitatively, the intensity of north-easterly trade winds is reduced by 13% in the northern hemisphere based on the MMM, leading to negative and positive wind stress curl anomalies over the tropical (equator to 10°N) and subtropical (10°N to 30°N) regions, respectively. Such a wind change pattern is consistent with the pattern of SST changes. The latter exhibits an El Niño-like warming with asymmetrical warming in the equatorial Pacific and greater SST anomalies over 3°C at cold tongue. [*Kug et al.*, 2011; *Song and Zhang*, 2014; *Cai et al.*, 2014].

As to the transport of the NKM system, the MMM volume transport of NEC, MC, and KC are 39.3 Sv, 22.2 Sv, and 17.9 Sv, respectively (Figure 2a). Although the magnitude of the transport is slightly weaker than observations or reanalysis products [*Qu et al.*, 1998; *Zhai et al.*, 2014], these values are still in a reasonable range given that the resolution of ocean models in CMIP5 is relatively coarse and cannot adequately resolve the narrow western boundary currents. For the projected changes, most models show a significant decrease of NKM transport (Figure 2d), with a MMM reduction of 3.0 Sv (7.7%), 2.0 Sv (10%), and 1.3 Sv (7.4%) for NEC, MC, and KC. The slowdown of NKM is supposed to be related to the weakened north-easterly trade winds that directly determine the total volume transport of NEC under global warming (El Niño-like warming pattern in the tropical Pacific).

It should be noted that this slow-down feature is not analogous to NKM interannual variabilities modulated by ENSO [e.g., *Kim et al.*, 2004; *Kashino et al.*, 2005, 2009; *Chen et al.*, 2015]; i.e., the MC strengthens and the KC weakens associated with the northward shift of NBL during the El Niño event and vice versa during the La Niña event. To get plausible explanations for this disparity, we compared the wind stress curl anomalies during the El Niño event and global warming scenario. During the El Niño event (Figure S1a in the supporting information), there is a significant positive wind stress curl anomaly located to the west of date line, which will induce anticlockwise circulation in the western Pacific, thus favoring enhanced MC, weakened KC, and the associated northward shift of the NBL. However, under the global warming scenario, the low-latitude Pacific Ocean is dominated by a robust basin-wide weakening of the north-easterly trade winds and the associated negative/positive wind stress curl anomalies over tropical/subtropical part of the low-latitude Pacific (Figure S1b). Such kind of changes in the wind stress curl will decrease the total transport of MC and KC according to Sverdrup balance.

The MMM NBL derived from historical runs is 14.5°N (Figure 2b), basically consistent with the mean position obtained from observations [*Qu and Lukas*, 2003; *Yaremchuk and Qu*, 2004; *Qiu and Chen*, 2010], reanalysis products, and numerical models [*Kim et al.*, 2004; *Chen and Wu*, 2012]. The MMM latitude of the zonally integrated zero line of the wind stress curl (140°E–120°W, hereinafter we use WCL for short) is 15.6°N (Figure 2b), which is 1.1° more northward than the NBL. According to the Sverdrup theory, the NEC should bifurcate at the latitude where there are no western boundary currents compensating the zero basin-averaged interior flow. The slight difference in their mean positions is likely due to the fact that the bifurcation is not vertically

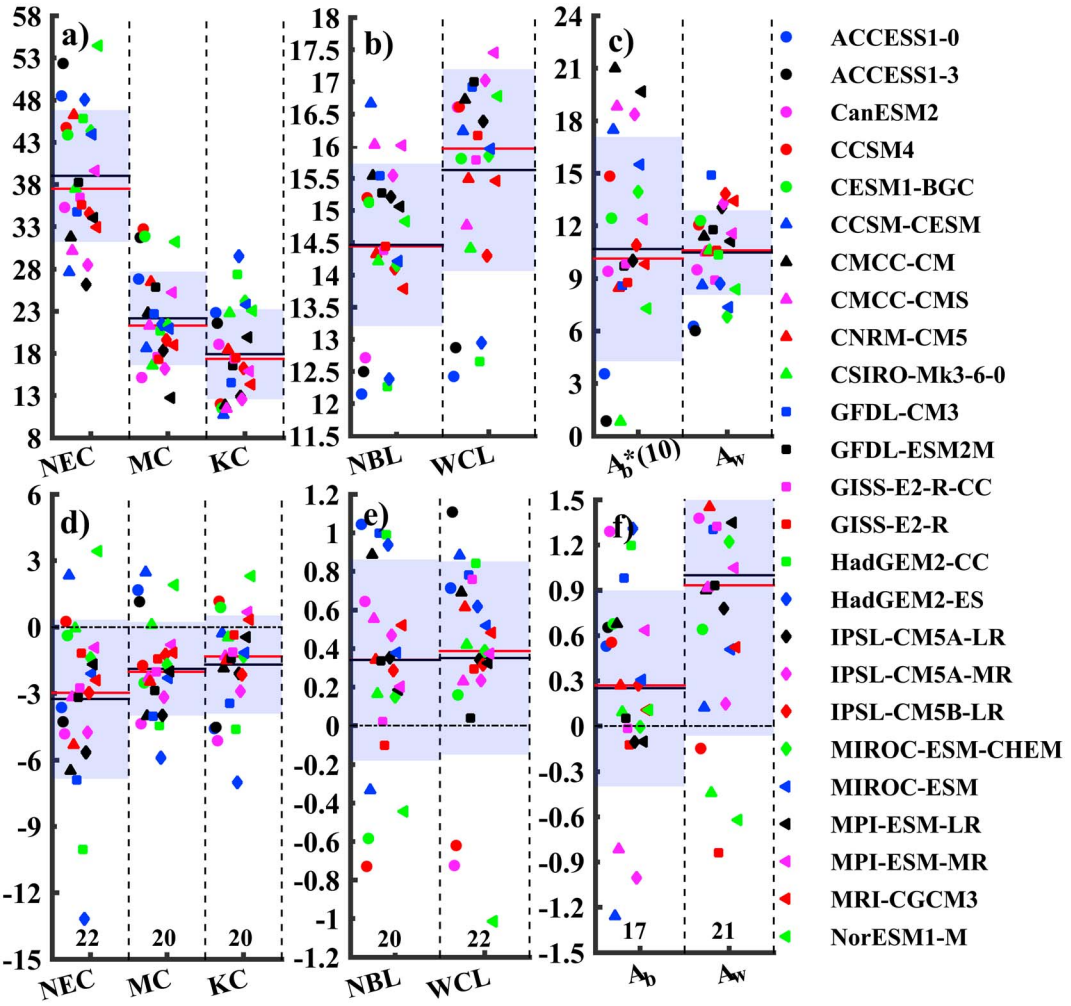

Figure 2. (a) Mean transport of NKM (Sv) system, (b) mean NBL (°N) and WCL (°N), and (c) seasonal migration of the NBL (A_b, unit: degree) and the WCL (A_w, unit: degree) from CMIP5 historical runs (1951–2000). (d–f) Same as Figures 2a–2c but for their projected changes (2051–2100 minus 1951–2000). A_b in Figure 2c is multiplied by 10 for clarity. Values at bottom of Figures 2d–2f denote the number of models (25 in total) that are in agreement with the sign of statistically mean value. Based on binomial distribution, agreement of 17, 18, 20, and 22 models (out of 25) corresponds to significance levels of 90%, 94%, 98%, and 99%, respectively. The black and red line are MMM and multimodel median, respectively, and the blue shading area shows the standard deviation.

uniform but characterized by a significant northward tilting with increasing depth. So it is possible that the upper 400 m mean NBL is located to the south of the WCL. The correlation coefficient between the NBL and WCL of 25 models is 0.88 (Figure 3b). Furthermore, both WCL and NBL exhibit northward shift under the global warming scenario with their magnitudes (0.35° for WCL and 0.34° for NBL) close to each other (Figure 2e). These facts provide evidence for the validity of Sverdrup dynamics in linking NBL with WCL on long timescales [*Chen and Wu*, 2012].

In addition to weakening the NKM transport, the slowdown of north-easterly trade winds also induces the alternation of the wind stress curl pattern, particularly the zero wind stress curl line. It is therefore necessary to further examine the distribution of the changes in the zero wind stress curl line. Figure 3a shows the projected change of the latitude of zero wind stress curl as a function of longitude. The projected WCLs do not uniformly shift northward. For the MMM, there is a significant northward shift (1.4°) in the western Pacific and southward shift (1.1°) to the east of 140°W. Although there exists large local deviations in WCL among 25 models, the overall change in the zero wind stress curl line is principally consistent with the wind stress pattern; that is, weakened north-easterly trade winds lead to positive wind stress curl in

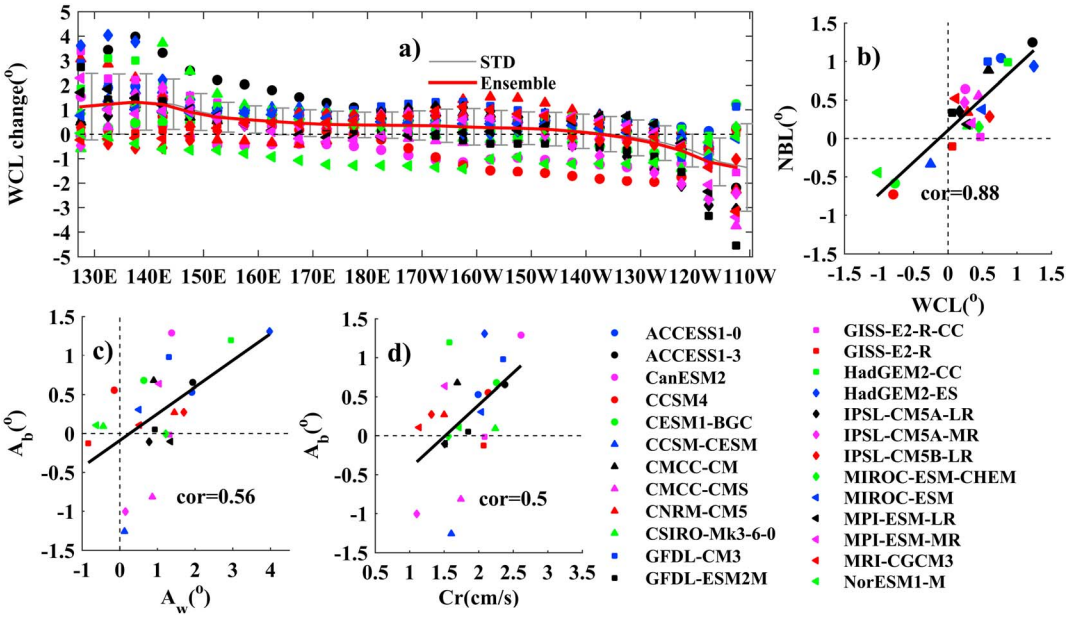

Figure 3. (a) Zonal distribution of model-projected change in WCL, and the grey lines represent the standard deviation. (b) Scatterplot of projected change of NBL and WCL for 25 CMIP5 models. (c) Scatterplot of projected change of A_b and A_w for 25 CMIP5 models. (d) Scatterplot of projected change of A_b and C_R for 25 CMIP5 models. The intermodel correlation is tested by a Monte Carlo simulation ($p < 0.01$).

the west and negative wind stress curl in the east (note that the mainstream of the trade winds presents a southwest-northeast orientation).

3.2. Projected Changes of the Seasonal Cycle

In addition to the mean state, the seasonal cycles of the NKM system also undergo discernible changes under global warming. In this part, we will mainly assess how much the seasonal variations of the NBL will change under global warming, particularly its amplitude of seasonal south-north migration (A_b). It is shown in Figure 2c that the MMM seasonal south-north migration of the WCL (A_w) and A_b over the historical period of 1951–2000 is 10.5° and 1.1°, respectively. These values are comparable to those derived from the observations and ocean reanalysis [e.g., *Qiu and Lukas*, 1996; *Qu and Lukas*, 2003; *Kim et al.*, 2004; *Chen and Wu*, 2011, 2012], indicating a good performance in simulating the seasonal variations of the NBL by the CMIP5 models. Compared to the historical state, there is a significant increase for both A_b (0.3°, 30%) and A_w (1.0°, 10%) (Figure 2f). Such an increase is on the same order in magnitude as the amplitude of A_b (0.8°) and A_w (3°) at the interannual timescale [*Chen and Wu*, 2012], implying that the change of seasonal variations of the NBL under global warming might exert remarkable impacts on regional circulation/climate and even the fisheries [*Kimura et al.*, 2001].

To further illustrate the significant change of A_b and A_w under global warming, we filter out the interannual/decadal variations in A_b and A_w by applying a 21 year running seasonal mean to the time series of A_b and A_w. Figures 5a and 5b show a robust increase of A_b from 1.3° in 1951 to 1.6° in 2100, which is mostly due to more migration to the north at its northernmost position in winter, and a robust increase of A_w from 10.2° in 1951 to 11.4° in 2100. It should be noted that A_b shares the same increasing pattern with A_w, implying that the changes in A_b can be deduced from the overall change of the basin-wide wind forcing (note that the correlation coefficient between the A_b and A_w of 25 models is 0.56; see Figure 3c). However, previous studies also highlighted the role of internal oceanic adjustment, i.e., baroclinic Rossby wave propagation in determining the seasonal variations of the NEC bifurcation in addition to the external wind stress forcing. Specifically, faster wave speed leads to larger seasonal migration [*Qiu and Lukas*, 1996; *Qu and Lukas*, 2003; *Chen and Wu*, 2011, 2012]. So it is noteworthy to check the possible relationship between the wave speed and seasonal migration. For this sake, we calculated the first baroclinic Rossby wave speed averaged over the region of

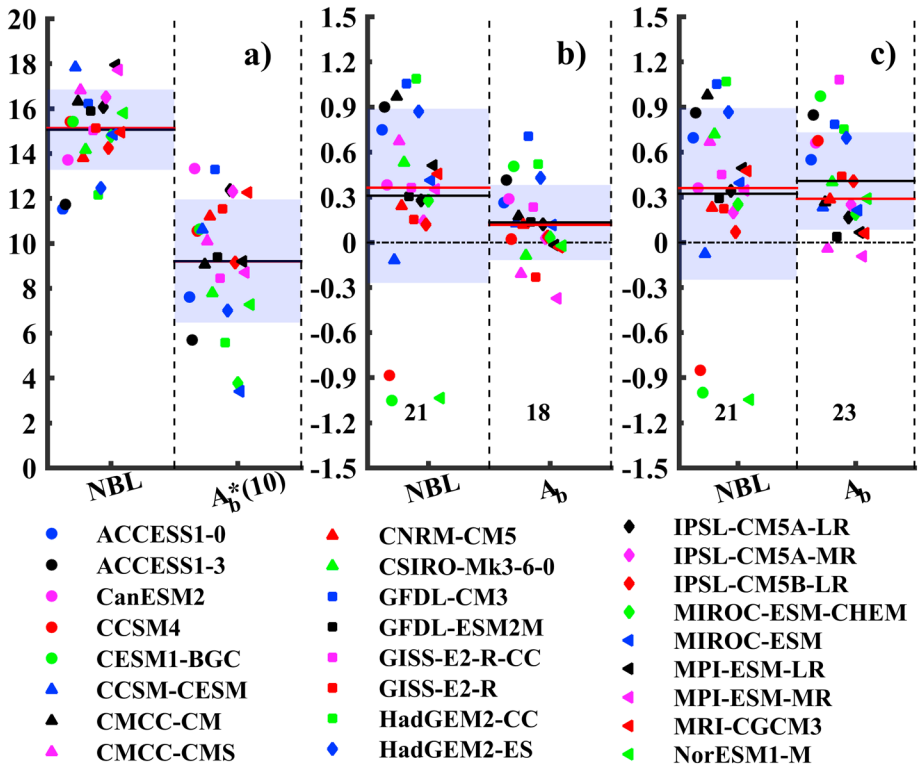

Figure 4. Results for three groups of runs derived from the 1.5-layer nonlinear reduced-gravity ocean model. (a) Mean position of NBL (°N) and its seasonal amplitude A_b (°) from R1. (b) Projected changes of the NBL and A_b (R2 minus R1). (c) Projected changes of the NBL and A_b (R3 minus R1). Values at the bottom of each column in Figures 4b and 4c denote the number of models (25 in total) that are in agreement with the sign of the changes. Based on binomial distribution, agreement of 17, 18, 20, and 22 models (out of 25) corresponds to significance levels of 90%, 94%, 98%, and 99%, respectively. The black and red line are MMM and multimodel median, respectively, and the blue shading area shows the standard deviation.

8°N–18°N and 140°E–70°W (hereinafter we use C_R for short) based on the method suggested by *Saenko* [2006] and found that there are good intermodel correlation between the A_b and C_R (correlation coefficient is 0.50; Figure 3d). As the phase speed of baroclinic Rossby wave is closely related to the upper ocean stratification that is believed to be intensified in a warmer climate [*Capotondi et al.*, 2012; *Ganachaud et al.*, 2013], it will be of great importance to further explore respective contribution of the amplified zero wind stress curl line migration and intensified upper ocean stratification to the elevated seasonal migration of NBL under global warming.

4. Role of Wind Forcing and Ocean Stratification

In this section, we employ a 1.5-layer nonlinear reduced-gravity Pacific basin model to assess the role of wind forcing and ocean stratification in favoring the amplified seasonal migration of the NEC bifurcation. The reader can refer to *Chen and Wu* [2011] for more details about the model. Three groups of model runs are conducted. R1 is driven by the wind stress under current climate with stratification $\Delta\rho = 3$ kg m^{-3}; R2 is driven by the wind stress under RCP8.5 scenario with the same stratification as R1. R3 is driven by the wind stress under RCP8.5 scenario along with the increased stratification $\Delta\rho = 3.5$ kg m^{-3}. Results show that this simple model can adequately capture the mean and seasonal cycle of NBL (Figure 4a). Specifically, the MMM position of NBL and its seasonal migration amplitude are 15.0°N and 0.92°, in good agreement with recent observations and modeling studies [e.g., *Yaremchuk and Qu*, 2004; *Chen and Wu*, 2011; *Yang et al.*, 2013; *Zhai et al.*, 2014].

For R2 and R3, it is shown in Figures 4b and 4c that the northward shifts of modeled NBL in each run are almost the same (0.36°), suggesting again that the projected changes in the mean position of NEC

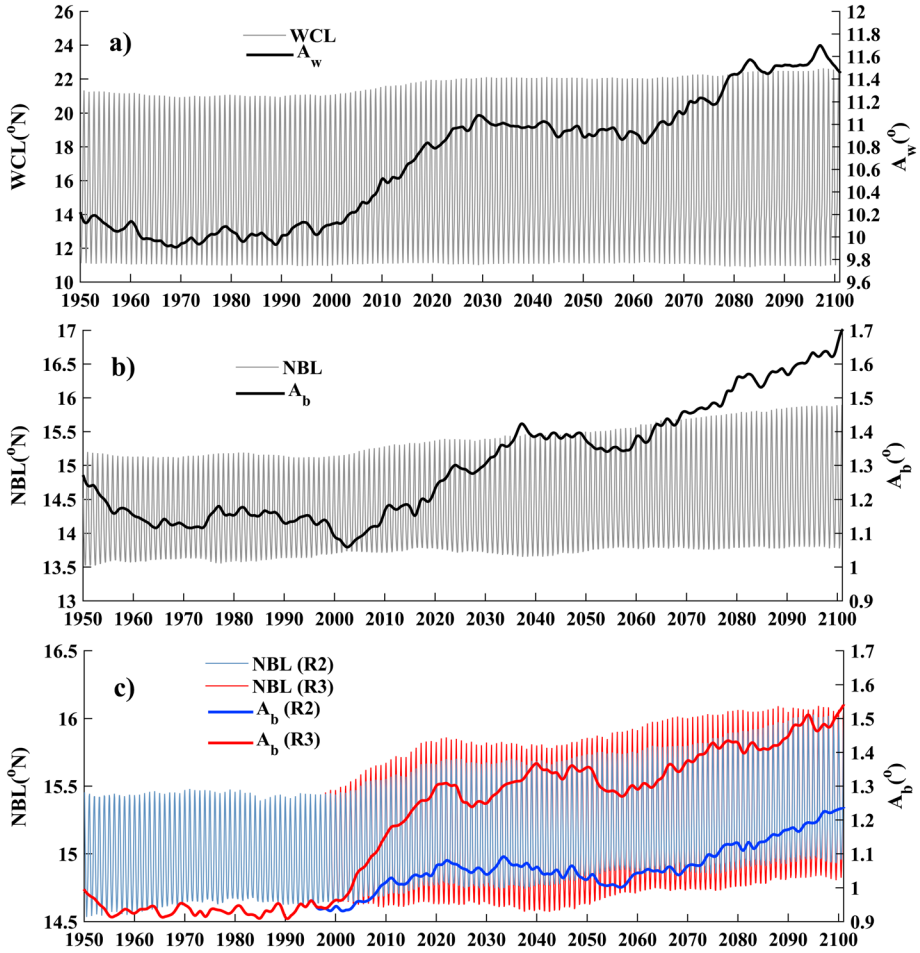

Figure 5. MMM time series with 21 year running seasonal mean (thin) and its seasonal amplitude (bold) of (a) WCL and (b) NBL derived from CMIP5 models. (c) Same as Figure 5b but from the 1.5-layer nonlinear reduced-gravity ocean model runs (blue for R2 and red for R3).

bifurcation are merely determined by the wind stress changes with the enhanced stratification in the upper ocean playing a negligible role. However, we note in Figures 4b and 4c that the changes in A_b are different in R2 (0.14°) and R3 (0.29°), indicating that an enhanced stratification and thus a faster speed of first-mode baroclinic Rossby waves contribute equally to the amplified seasonal migration of the NBL. According to the study by *Chen and Wu* [2012], the incremental NBL's amplitude is not only fully controlled by the projected wind forcing but also modulated by the increased baroclinic adjustment. We further apply a 21 year running seasonal mean to the time series of A_b from the above two group runs. It is shown in Figure 5c that the projected change of A_b in R3 is twice the value in R2. This clearly indicates that the changes in the wind forcing and intensified upper ocean stratification are equally important in amplifying the seasonal migration of the NBL in the future climate.

5. Summary

The response of the low-latitude north-western Pacific circulation to global warming is investigated by analyzing 25 CMIP5 models and a 1.5-layer nonlinear reduced-gravity Pacific basin model. The summary of this study is as follows.

1. For the MMM, the projected changes of the WCL and NBL both exhibit northward shift under global warming (WCL shifts northward by 0.35° and NBL shifts northward by 0.34°), and the linear correlation between them is 0.88 from 25 models, implying the validity of Sverdrup dynamics in linking NBL with WCL on long timescale.

2. Most models show a significant decrease in the transport of NKM, with a reduction of 3.0 Sv (7.7%), 1.3 Sv (7.4%), and 2.0 Sv (10%) for the MMM. This reduction is attributed to the weakened north-easterly trade winds.
3. On the seasonal timescale, there is a robust increase in both A_b (0.3°, 30%) and A_w (1.0°, 10%). Based on a 1.5-layer reduced gravity model, it is indicated that enhanced stratification of the upper ocean and intensified south-north migration of the zero wind stress curl line act equally important in amplifying the seasonal migration of the NEC bifurcation.

In this paper, we have only highlighted the wind-driven response of the circulation to the global warming, which is believed to be associated with the El Niño-like SST response and the projected wind changes [*Xie et al.*, 2010]. However, the future changes of the NKM transport as well as the NBL are not analogous to their interannual variabilities (e.g., during El Niño events) because the changes of the wind stress pattern are different. We will not discuss in-depth the detailed mechanisms for the projected SST and wind changes here, and this issue will be explored in our next study.

Acknowledgments
This research is supported by the National Natural Science Foundation of China (41622602, 41521091, U1606402, and 41306001), the National Basic Research Program of China (2013CB956200), the Strategic Priority Research Program of the Chinese Academy of Sciences (XDA11010101), and the Global Change Project (GASI-03-01-01-05). The authors are grateful to the discussions with Bo Qiu and Zhao Jing. CMIP5 model outputs can be downloaded at http://cmip-pcmdi.llnl.gov/cmip5/.

References

Cai, W., et al. (2014), Increasing frequency of extreme El Niño events due to greenhouse warming, *Nat. Clim. Change*, *4*(2), 111–116, doi:10.1038/NCLIMATE2100.

Capotondi, A., M. A. Alexander, N. A. Bond, E. N. Curchitser, and J. D. Scott (2012), Enhanced upper ocean stratification with climate change in the CMIP3 models, *J. Geophys. Res.*, *117*, C04031, doi:10.1029/2011JC007409.

Chen, Z., and L. Wu (2011), Dynamics of the seasonal variation of the North Equatorial Current bifurcation, *J. Geophys. Res.*, *116*, C02018, doi:10.1029/2010JC006664.

Chen, Z., and L. Wu (2012), Long-term change of the Pacific North Equatorial Current bifurcation in SODA, *J. Geophys. Res.*, *117*, C06016, doi:10.1029/2011JC007814.

Chen, Z., L. Wu, B. Qiu, L. Li, D. Hu, C. Liu, F. Jia, and X. Liang (2015), Strengthening Kuroshio observed at its origin during November 2010 to October 2012, *J. Geophys. Res. Oceans*, *120*, 2460–2470, doi:10.1002/2014JC010590.

Ganachaud, A., A. S. Gupta, J. N. Brown, K. Evans, C. Maes, L. C. Muir, and F. S. Graham (2013), Projected changes in the tropical Pacific Ocean of importance to tuna fisheries, *Clim. Change*, *119*(1), 163–179, doi:10.1007/s10584-012-0617-z.

Gordon, A. L., R. D. Susanto, and K. Vranes (2003), Cool Indonesian throughflow as a consequence of restricted surface layer flow, *Nature*, *425*(6960), 824–828, doi:10.1038/nature02038.

Gu, D., and S. G. H. Philander (1997), Interdecadal Climate Fluctuations That Depend on Exchanges Between the Tropics and Extratropics, *Science*, *275*(5301), 805–807, doi:10.1126/science.275.5301.805.

Hsin, Y. C., and B. Qiu (2012), Seasonal fluctuations of the surface North Equatorial Countercurrent (NECC) across the Pacific basin, *J. Geophys. Res.*, *117*, C06001, doi:10.1029/2011JC007794.

Hu, D., and M. Cui (1989), The western boundary current in the far western Pacific ocean, paper presented at Proc. of the Western Pacific Int. Meeting and Workshop on TOGA-COARE, ORSTOM, Noumea, New Caledonia.

Hu, D., et al. (2015), Pacific western boundary currents and their roles in climate, *Nature*, *522*(7556), 299, doi:10.1038/nature14504.

Johnson, G. C., and M. J. Mcphaden (1999), Interior Pycnocline flow from the subtropical to the equatorial Pacific Ocean, *J. Phys. Oceanogr.*, *29*(12), 3073–3089, doi:10.1175/1520-0485(1999)029<3073:IPFFTS>2.0.CO;2.

Kashino, Y., A. Ishida, and Y. Kuroda (2005), Variability of the Mindanao Current: Mooring observation results, *Geophys. Res. Lett.*, *32*, L18611, doi:10.1029/2005GL023880.

Kashino, Y., N. España, F. Syamsudin, K. J. Richards, T. Jensen, P. Dutrieux, and A. Ishida (2009), Observations of the North Equatorial Current, Mindanao Current, and Kuroshio current system during the 2006/07 El Niño and 2007/08 La Niña, *J. Oceanogr.*, *65*(3), 325–333, doi:10.1007/s10872-009-0030-z.

Kelly, K. A., et al. (2010), Western boundary currents and frontal air-sea interaction: Gulf stream and Kuroshio extension, *J. Clim.*, *23*(21), 5644–5667, doi:10.1175/2010JCLI3346.1.

Kim, Y. Y., T. Qu, T. Jensen, T. Miyama, H. Mitsudera, H.-W. Kang, and A. Ishida (2004), Seasonal and interannual variations of the North Equatorial Current bifurcation in a high-resolution OGCM, *J. Geophys. Res.*, *109*, C03040, doi:10.1029/2003JC002013.

Kimura, S., T. Inoue, and T. Sugimoto (2001), Fluctuation in the distribution of low-salinity water in the North Equatorial Current and its effect on the larval transport of the Japanese eel, *Fish. Oceanogr.*, *10*, 51–60, doi:10.1046/j.1365-2419.2001.00159.x.

Kug, J., K. P. Sooraj, F. Jin, Y. Ham, and D. Kim (2011), A possible mechanism for El Niño-like warming in response to the future greenhouse warming, *Int. J. Climatol.*, *31*(10), 1567–1572, doi:10.1002/joc.2163.

Kwon, Y., M. Alexander, N. Bond, C. Frankignoul, H. Nakamura, B. Qiu, and L. Thompson (2010), Role of the Gulf Stream and Kuroshio–Oyashio systems in large-scale atmosphere–ocean interaction: A review, *J. Clim.*, *23*, 3249–3281, doi:10.1175/2010JCLI3343.1.

Lukas, R., et al. (1991), Observations of the Mindanao Current during the western equatorial Pacific Ocean circulation study, *J. Geophys. Res.*, *96*(C4), 7089–7104, doi:10.1029/91JC00062.

Lukas, R., T. Yamagata, and J. P. McCreary (1996), Pacific low-latitude western boundary currents and the Indonesian throughflow, *J. Geophys. Res.*, *101*(C5), 12,209 –12,216, doi:10.1029/96JC01204.

Osamu, A., and K. Akio (2004), Comparison of local precipitation–SST relationship between the observation and a reanalysis dataset, *Geophys. Res. Lett.*, *31*, L12206, doi:10.1029/2004GL020283.

Qiu, B., and S. Chen (2010), Eddy-mean flow interaction in the decadally modulating Kuroshio Extension system, *Deep Sea Res., Part II*, *57*, 1097–1110, doi:10.1016/j.dsr2.2008.11.036.

Qiu, B., and R. Lukas (1996), Seasonal and interannual variability of the North Equatorial Current, the Mindanao Current, and the Kuroshio along the Pacific western boundary, *J. Geophys. Res.*, *101*, 12,315–12,330, doi:10.1029/95JC03204.

Qu, T., and R. Lukas (2003), The bifurcation of the North Equatorial Current in the Pacific, *J. Phys. Oceanogr.*, *33*(1), 5–18, doi:10.1175/1520-0485(2003)033<0005:TBOTNE>2.0.CO;2.

Qu, T., M. Humio, and Y. Toshio (1998), On the western boundary currents in the Philippine Sea, *J. Geophys. Res.*, *103*, 7537–7548, doi:10.1029/98JC00263.

Rudnick, D., S. Jan, and C. Lee (2015), A new look at circulation in the western North Pacific, *Oceanography*, *28*(4), 16–23, doi:10.5670/oceanog.2015.77.

Saenko, O. A. (2006), Influence of global warming on Baroclinic Rossby radius in the ocean: A model intercomparison, *J. Clim.*, *19*(7), 1354, doi:10.1175/JCLI3683.1.

Sasaki, Y. N., S. Minobe, T. Asai, and M. Inatsu (2012), Influence of the Kuroshio in the East China Sea on the early summer (Baiu) rain, *J. Clim.*, *25*(19), 6627–6645, doi:10.1175/JCLI-D-11-00727.1.

Sen Gupta, A., A. Ganachaud, S. Mcgregor, J. N. Brown, and L. Muir (2012), Drivers of the projected changes to the Pacific Ocean equatorial circulation, *Geophys. Res. Lett.*, *39*, L09605, doi:10.1029/2012GL051447.

Sen Gupta, A., S. Mcgregor, E. Sebille, A. Ganachaud, J. N. Brown, and A. Santoso (2016), Future changes to the Indonesian Throughflow and Pacific circulation: The differing role of wind and deep circulation changes, *Geophys. Res. Lett.*, *43*, 1669–1678, doi:10.1002/2016GL067757.

Schönau, M. C., D. L. Rudnick, I. Cerovecki, G. Gopalakrishnan, B. D. Cornuelle, J. L. McClean, and B. Qiu (2015), The Mindanao current, *Oceanography*, *28*(4), 34.

Song, X., and G. J. Zhang (2014), Role of climate feedback in El Niño-like SST response to global warming, *J. Clim.*, *27*(19), 7301–7318, doi:10.1175/JCLI-D-14-00072.1.

Sprintall, J., et al. (2014), The central role of the Indonesian Seas and throughflow in the coupled ocean-climate system, *Nat. Geosci.*, *7*(7), 487–492, doi:10.1038/ngeo2188.

Wittenberg, A. T., G. A. Vecchi, and B. J. Soden (2006), Global warming and the weakening of the tropical circulation, AGU Fall Meeting (Vol.20, pp.1529–1530). AGU Fall Meeting Abstracts, doi:10.1175/JCLI4258.1.

Wu, R., and S. P. Xie (2013), On equatorial pacific surface wind changes around 1977: NCEP-NCAR reanalysis versus COADS observations, *J. Clim.*, *16*(1), 167–173, doi:10.1175/1520-0442(2003)016<0167:OEPSWC>2.0.CO;2.

Xie, S. P., et al. (2010), Global Warming Pattern Formation: Sea Surface Temperature and Rainfall*, *J. Clim.*, *23*(4), 966–986, doi:10.1175/2009JCLI3329.1.

Yang, J., X. Lin, and D. Wu (2013), On the dynamics of the seasonal variation in the South China Sea throughflow transport, *J. Geophys. Res. Oceans*, *118*, 6854–6866, doi:10.1002/2013JC009367.

Yaremchuk, M., and T. Qu (2004), Seasonal variability of the large-scale currents near the coast of the Philippines*, *J. Phys.Oceanogr.*, *34*(4), 844–855, doi:10.1175/1520-0485(2004)034<0844:SVOTLC>2.0.CO;2.

Zhai, F., Q. Wang, F. Wang, and D. Hu (2014), Variation of the North Equatorial Current, Mindanao Current, and Kuroshio Current in a high-resolution data assimilation during 2008–2012, *Adv. Atmos. Sci.*, *31*(6), 1445–1459, doi:10.1007/s00376-014-3241-1.